

## Supporting Information

### **Sodium-ion-stabilized $2 \times 4$ tunnel manganese oxide nanorods as cathodes for high-performance aqueous zinc-ion batteries**

Shuling Liu\*<sup>1</sup>; Ruirui Teng<sup>1</sup>; Xiangyang Wei<sup>1</sup>; Yupei Li<sup>1</sup>; Zixiang Zhou<sup>1</sup>; Xiaoqiang Shi<sup>1</sup>;  
Jiebing Li<sup>2</sup>; Jianbo Tong\*<sup>1</sup>

<sup>1</sup>*College of Chemistry and Chemical Engineering, Shaanxi University of Science and Technology,*

*Xi'an 710021, China*

<sup>2</sup>*Shaanxi Applied Physics and Chemistry Research Institute*

\*Corresponding author.

E-mail address: [liushuling@sust.edu.cn](mailto:liushuling@sust.edu.cn)

[tongjianbo@sust.edu.cn](mailto:tongjianbo@sust.edu.cn)

## **Table of Content:**

1. EDX
2. ICP
3. XRD
4. SEM
5. Electrochemistry
6. BET
7. XRD
8. Crystal data

## 1. EDX

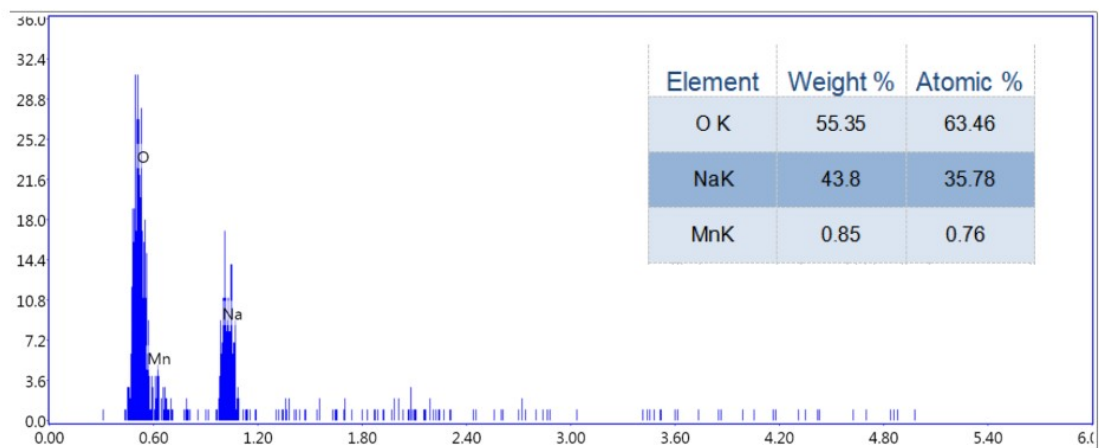


**Fig. S1** EDX of the  $\text{Na}_{0.4}\text{MnO}_2$  and the corresponding elemental content .

## 2. ICP-AES

ICP-AES	Atomic Percentage (%)	
	Na	Mn
$\text{Na}_{0.4}\text{MnO}_2$	28.57	71.43
Na-birnessite	10.77	89.23

**Table S1** Contents of the manganese oxide

### 3. XRD

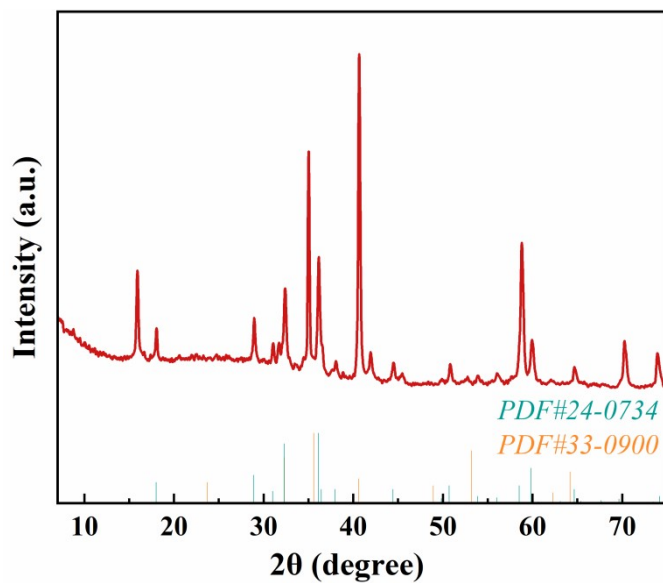


**Fig. S2** XRD of the  $\text{Na}_{0.4}\text{MnO}_2$  after 550 °C

After annealed at 550 °C , the  $\text{Na}_{0.4}\text{MnO}_2$  powders is converted into  $\text{Mn}_2\text{O}_3$  and  $\text{Mn}_3\text{O}_4$ . The  $\text{Na}_{0.4}\text{MnO}_2$  powder was annealed at 550 °C for 2h and XRD patterns are shown in **Fig. S2**.

### 4. SEM

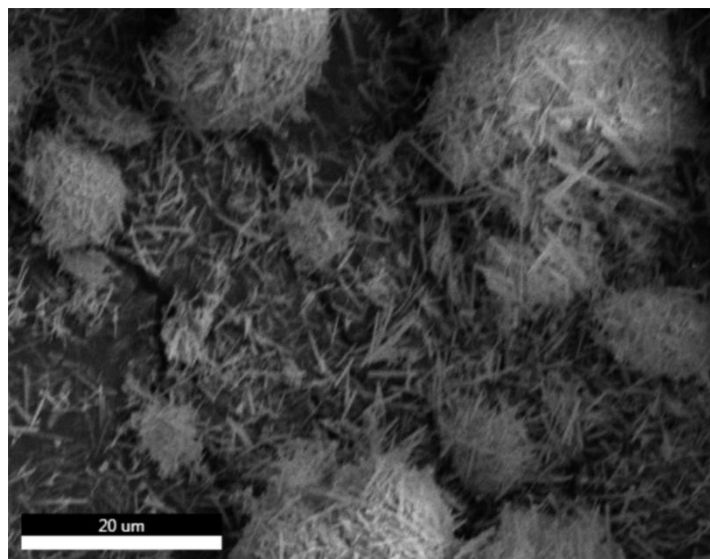


**Fig. S3** SEM of the  $\text{Na}_{0.4}\text{MnO}_2$

## 5. Electrochemistry

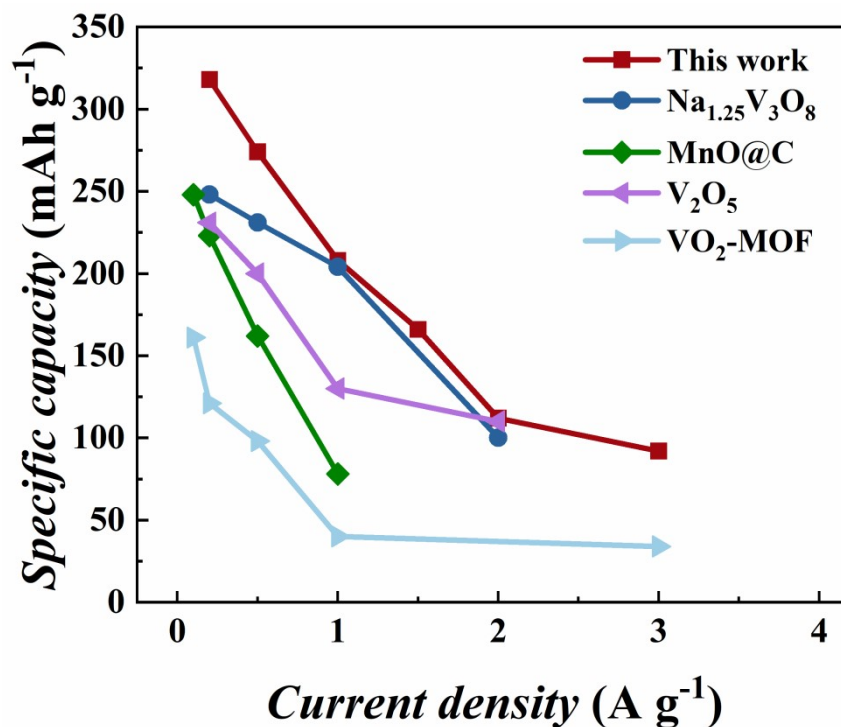


**Fig. S4** Compared with other ZIBs Mn-based electrodes previously reported, the specific capacity (stable capacity) of Na<sub>0.4</sub>MnO<sub>2</sub> is higher at different current densities.

[1] Zhao Yanming, Liao Jinhui. Rubidium-doped Na<sub>1.25</sub>V<sub>3</sub>O<sub>8</sub> Electrochemical properties of nanorods as cathode materials for zinc-ion batteries[J].Journal of South China University of Technology:Natural Science Edition, 2023, 51(3):63-73.)

[2] Guo Pingchun, Han Xing, Jiang Hedong, et al. Research on vanadium-based metal-based organic framework materials as cathode materials for aqueous zinc-ion batteries[J].Acta Ceramic Sinica, 2023, 44(5):920-927.)

[3] Huang Yongfeng, Huang Wenting, Liu Wenbao, et al. Energy storage mechanism and capacity attenuation reasons of Zinc-ion battery cathode material V<sub>2</sub>O<sub>5</sub>[J].Chem. J. Chinese Universities, 2020, 41(8):7.

[4] Ma Qiuchen, Liu Jun. MnO@C for research on cathode materials for zinc-ion batteries[J].Mining and Metallurgical Engineering, 2021, 41(1):4.

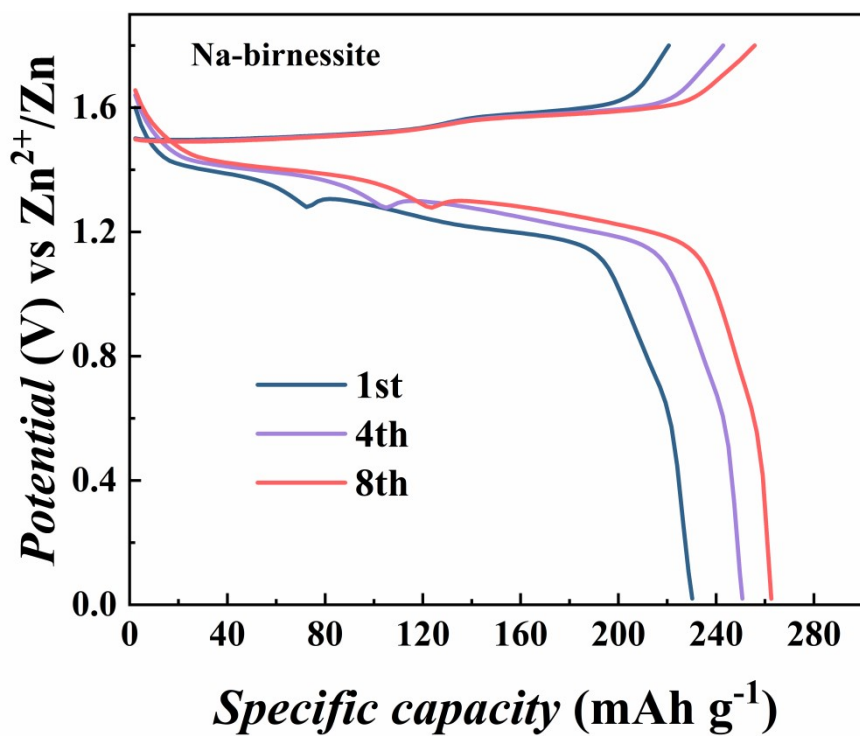


Fig.S5 GCD profiles of the Na-birnessite electrode obtained at  $0.2 \text{ A g}^{-1}$ .

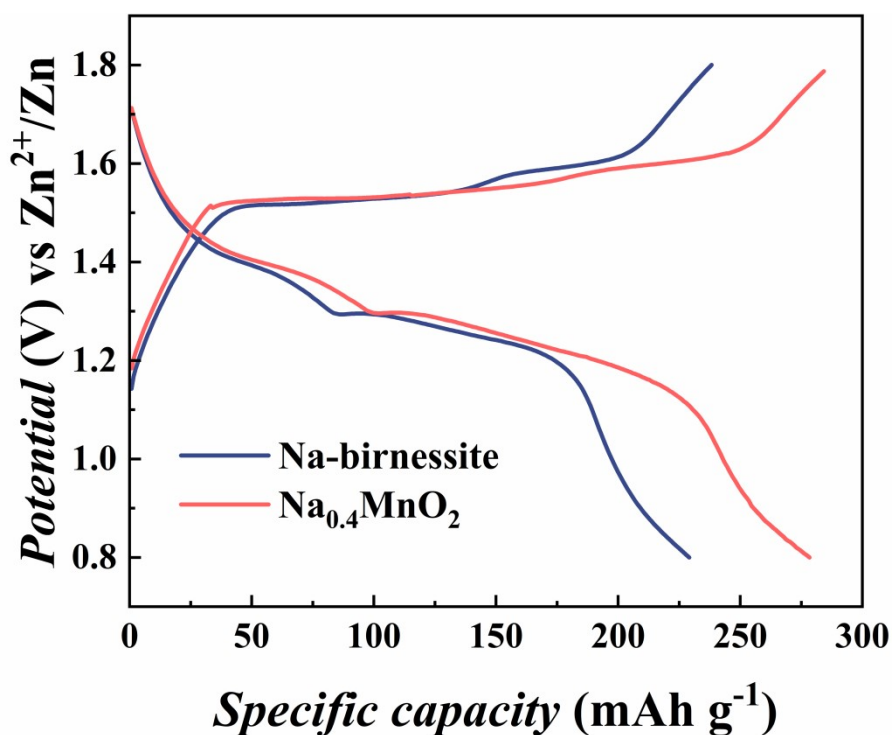
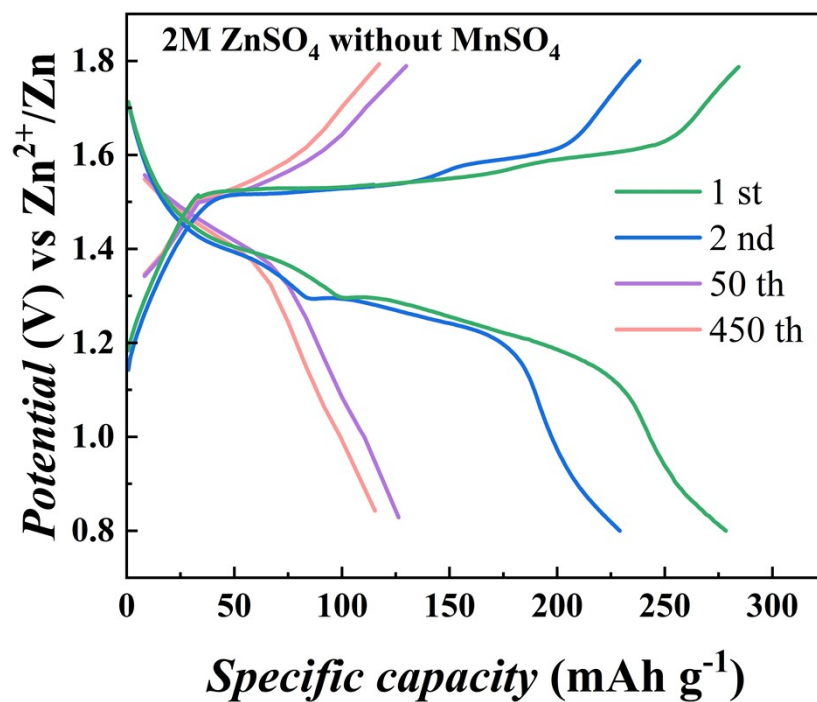
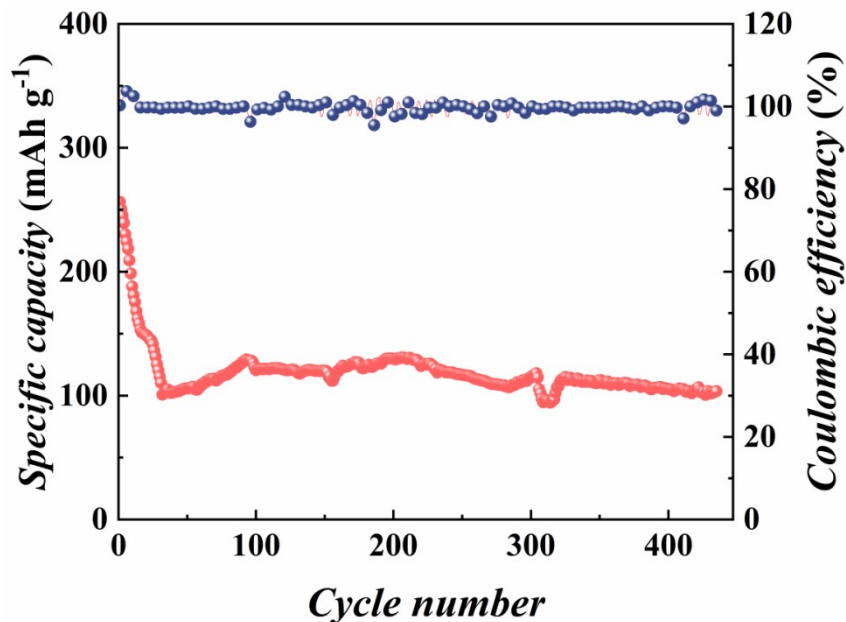


Fig.S6 Comparison of GCD profiles between  $\text{Na}_{0.4}\text{MnO}_2$  and Na-birnessite at  $0.2 \text{ A g}^{-1}$ .



**Fig.S7** GCD profiles of the  $\text{Na}_{0.4}\text{MnO}_2$  electrode obtained in aqueous electrolyte (2 M  $\text{ZnSO}_4$ ) at a scan of  $0.2 \text{ A g}^{-1}$ .



**Fig.S8** Cycling performance of the  $\text{Na}_{0.4}\text{MnO}_2$  at  $0.2 \text{ A g}^{-1}$  in aqueous electrolyte (2 M  $\text{ZnSO}_4$ ).

the battery was tested for 450 cycles at  $0.2 \text{ mA g}^{-1}$  in **Fig S8**. It was found that the capacity of the  $\text{Na}_{0.4}\text{MnO}_2$  sample gradually decreased from  $258 \text{ mAh g}^{-1}$  to  $114 \text{ mAh g}^{-1}$  when without  $\text{Mn}^{2+}$  was added to the electrolyte, the capacity retention rate is only 44.1%.



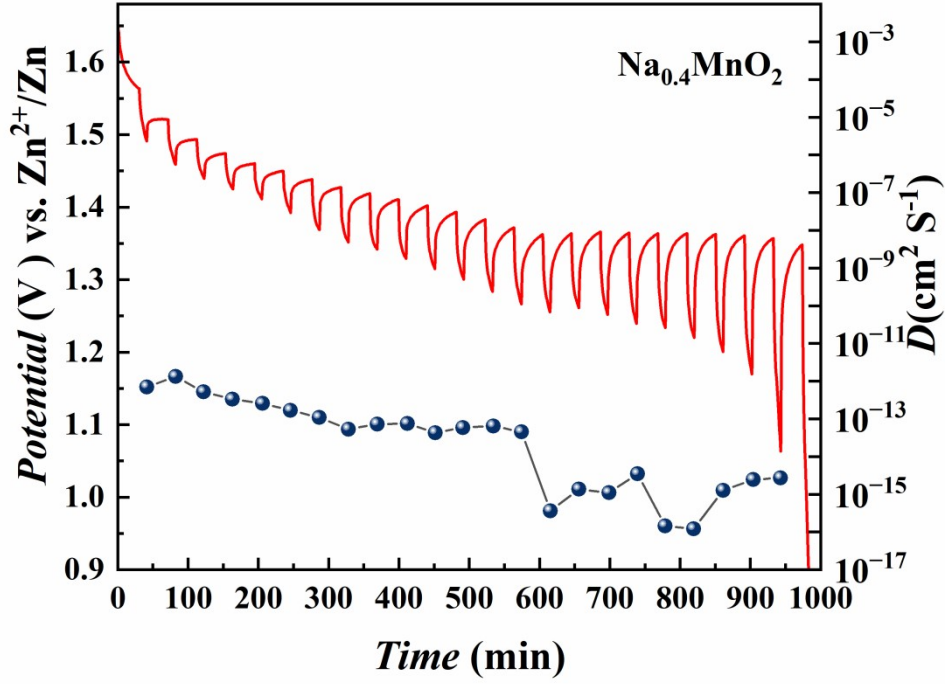


**Fig S10.** GITT curve and the corresponding diffusion coefficients in discharge process of the ZIB

with  $\text{Na}_{0.4}\text{MnO}_2$

The GITT measurement of  $\text{Na}_{0.4}\text{MnO}_2$  electrode was conducted at the current density of  $0.1 \text{ A g}^{-1}$ . The charging time and rest time are 10 min and 30 min, respectively. When discharged to 1.45 V, the diffusion coefficient of  $\text{H}^+$  is  $7.52 \times 10^{-13} \text{ cm}^2 \text{ s}^{-1}$ , and when discharged to 1.35 V, the diffusion rate of  $\text{Zn}^{2+}$  is  $6.49 \times 10^{-15} \text{ cm}^2 \text{ s}^{-1}$ . As shown in Fig. S10, the voltage ( $\Delta E_\tau$ ) exhibits a linear behavior with the square root of the titration time ( $\tau^{1/2}$ ). Therefore, the diffusion coefficient can be calculated based on the Equation (S3):

$$D = \frac{4}{\pi} \left( \frac{m_B V_M}{\tau M_B A} \right)^2 \left( \frac{\Delta E_S}{\Delta E_\tau} \right)^2 \quad (\text{S4})$$

Here,  $\tau$  is the constant pulse time 30 min,  $m_B$  is the mass of the active material,  $V_M$  is the molar volume,  $m_B$  is the molecular weight,  $A$  is the surface area of electrode with electrode, and  $\Delta E_\tau$  is the difference of stabilized open-circuit for the corresponding step. Accordingly, in this  $\text{Na}_{0.4}\text{MnO}_2$  battery, the relationship between diffusion coefficient and  $(\Delta E_S/\Delta E_\tau)^2$  can be described as Eq. S4:

$$\frac{D_1}{D_2} = \frac{\left(\frac{\Delta E_{S,1}}{\Delta E_{\tau,1}}\right)^2}{\left(\frac{\Delta E_{S,2}}{\Delta E_{\tau,2}}\right)^2} \quad (S5)$$

- [1] Heubner C, Schneider M, Michaelis A. SoC dependent kinetic parameters of insertion electrodes from staircase—GITT [J]. *Journal of Electroanalytical Chemistry*, 2016, 767: 18-23.
- [2] Deiss E. Spurious chemical diffusion coefficients of Li<sup>+</sup> in electrode materials evaluated with GITT [J]. *Electrochimica Acta*, 2005, 50(14): 2927-2932.

#### 6.BET

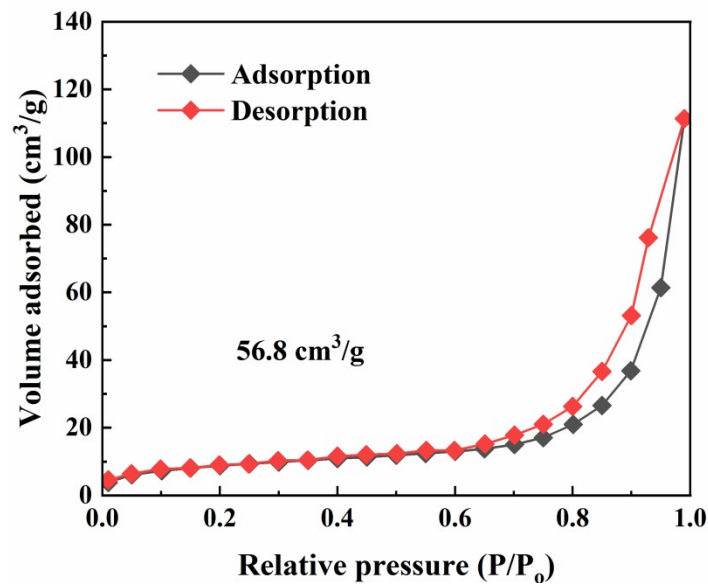


**Fig S11.** BET pattern of Na-birnessite sample

**Fig. S11** displays the BET results of Na-birnessite. The N<sub>2</sub> adsorption-desorption isothermal curve of Na-birnessite belongs to type II, which is a material with large pores or no pores.

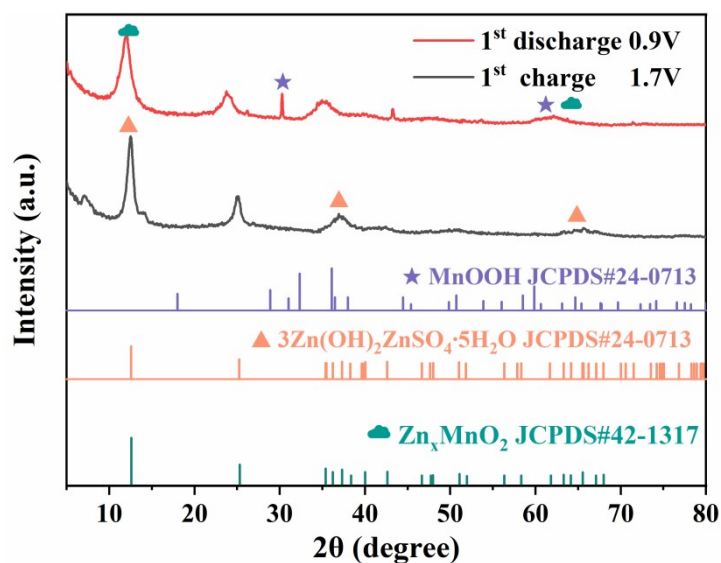


Fig .S12 the ex-situ XRD at different charge–discharge stages

The ex-situ XRD plots of the material in different charge/discharge states are shown in Fig.S12. These nanosheets are identified as  $\text{ZnSO}_4 \cdot 3\text{Zn}(\text{OH})_2 \cdot 5\text{H}_2\text{O}$  (BZSP), and its formation is associated with the increase in local pH induced by  $\text{H}^+$  insertion. At 1.7 V, the flakes gradually disappear, which is attributed to the conversion of BZSP to  $\text{ZnMn}_3\text{O}_7 \cdot 3\text{H}_2\text{O}$  as indicated by the XRD analysis in Fig. S12. In addition, MnOOH and  $\text{Zn}_x\text{MnO}_2$  phases are also detected from the fully discharged  $\text{Na}_{0.4}\text{MnO}_2$  anode(Fig. S12), During the first discharging stage at 0.9V, the intercalation of  $\text{Zn}^{2+}$  and  $\text{H}^+$  occurs in  $\text{Na}_{0.4}\text{MnO}_2$  to form layered  $\text{Zn}_x\text{MnO}_2$ , MnOOH and the byproduct BZSP.

- [1] Lee B, Seo H R, Lee H R, et al. Critical Role of pH Evolution of Electrolyte in the Reaction Mechanism for Rechargeable Zinc Batteries [J]. Chemsuschem, 2016.
- [2] Li Y, Li X, Duan H, et al. Aerogel-structured  $\text{MnO}_2$  cathode assembled by defect-rich ultrathin nanosheets for zinc-ion batteries [J]. Chemical Engineering Journal, 2022, 441: 136008-.
- [3] Sun W, Wang F, Hou S, et al. Zn/ $\text{MnO}_2$  battery chemistry with  $\text{H}^+$  and  $\text{Zn}^{2+}$  coinsertion [J]. Journal of the American Chemical Society, 2017, 139(29): 9775-9778.

Parameter	
Chemical formula	Na <sub>0.4</sub> MnO <sub>2</sub>
Space group	C2/m
Step scan increment (°)	0.03
2θ range (°)	5-80
a (Å)	14.28
b (Å)	2.84
c (Å)	23.84

Table 2. Crystal data for Na<sub>0.4</sub>MnO<sub>2</sub>.